

Available online at www.sciencedirect.com

ScienceDirect

journal homepage: www.journals.elsevier.com/oceanologia

SHORT COMMUNICATION

Effects of air-sea drag coefficient on estimating wind stress using wind statistics

Dag Myrhaug*, Hong Wang, Lars Erik Holmedal, Bernt J. Leira

Department of Marine Technology, Norwegian University of Science and Technology (NTNU), Trondheim, Norway

Received 23 November 2021; accepted 17 March 2022

Available online 31 March 2022

KEYWORDS

Wind stress;
Drag coefficient;
North Atlantic;
Northern North Sea;
Wind statistics;
Stochastic method

Abstract This article addresses the effects of the air-sea drag coefficient on estimation of wind stress based on wind statistics. This is achieved by applying the same wind stress parameterizations chosen by Wrobel-Niedzwiecka et al. (2019) together with mean wind speed statistics from three locations in the North Atlantic and one location in the Northern North Sea. The expected values and the variances of the wind stress are provided. This study is complementary to that of Wrobel-Niedzwiecka et al. (2019), also demonstrating different results depending on the drag coefficient formula used.

© 2022 Institute of Oceanology of the Polish Academy of Sciences. Production and hosting by Elsevier B.V. This is an open access article under the CC BY license (<http://creativecommons.org/licenses/by/4.0/>).

1. Introduction

Knowledge of the wind stress on the sea surface is important in order to understand the interaction between the atmosphere and the ocean as the air-sea interface represents their coupling by exchanging heat and momentum. This contributes to air-sea mixing processes which occur across the

ocean surface, and knowledge about these processes is crucial in climate and ocean studies. The wind shear stress enters in modelling and prediction of, for example, ocean surface waves, ocean currents and ocean circulations. The physical processes in the air-sea mixed layer are usually nonlinear depending on relevant air and sea parameters. Due to the lack of consistent theories on the exchange of the horizontal momentum between the air and the sea, parameterizations in terms of bulk formulae are often used by researchers when undertaking atmospheric and ocean studies.

Wrobel-Niedzwiecka et al. (2019) (hereafter referred to as WN19) studied the effect of some commonly used bulk formulae of the wind shear stress parameterized in terms of a drag coefficient and the mean wind speed (see Eq. (1)). They evaluated the dependence of the average monthly and annual wind stress values on the choice of drag coefficient using actual wind fields representing global satellite data

* Corresponding author at: Department of Marine Technology (NTNU), Otto Nielsen vei 10, NO-7491 Trondheim, Norway.

E-mail address: dag.myrhaug@ntnu.no (D. Myrhaug).

Peer review under the responsibility of the Institute of Oceanology of the Polish Academy of Sciences.



Production and hosting by Elsevier

from the North Atlantic and the European Arctic. Differences were obtained depending on the drag coefficient formula used. They used the formulae provided by Wu (1969, 1982), Garratt (1977), Yelland and Taylor (1996), Kalnay et al. (1996), Large and Yeager (2004), and Andreas et al. (2012) (see WN19 for more details related to these references as well as a review of the relevant literature).

The purpose of this article is to estimate the wind stress using the same shear stress bulk formulae as in WN19 together with mean wind speed statistics at four locations; three in the North Atlantic (NA) and one in the Northern North Sea (NNS). Thus, this study is complementary to that of WN19, also demonstrating different results depending on the drag coefficient formula used. WN19 found that the area average annual mean values of wind stress were smallest using the Andreas et al. (2012) formula and largest using the Wu (1969) formula which is different from the present results, i.e. the mean wind stress is largest using the Andreas et al. (2012) formula and smallest using the Wu (1969) formula or the Large and Yeager (2004) formula. The reason for this difference is unclear but it is probably related partly to how the wind data is used together with the drag coefficient formulae and partly to the use of global and local wind data. However, further studies are required to investigate this, which is beyond the scope of this article.

The article is organized as follows. This introduction is followed by providing the background of the wind stress bulk formulae used. Then the statistical properties of the wind stress using mean wind speed statistics are derived. Finally, a summary and the main conclusions are given.

2. Background

As referred to, WN19 made a review of some frequently used bulk formulae for the wind shear stress on the sea surface. Due to the lack of consensus on which formulae is the most reliable and as no consistent theory on the exchange of horizontal momentum between the atmosphere and the ocean exist in the literature these bulk formulae are adopted in the present study. For the sake of completeness the formulae are summarized here (see WN19 for more details).

The bulk formula for the wind shear stress on the sea surface is given as

$$\tau = \rho C_D U_{10}^2 \tag{1}$$

where ρ is the air density, C_D is the sea surface drag coefficient, and U_{10} is the mean wind speed 10 m above the sea surface. The friction velocity u_* is defined as $u_*^2 = \tau/\rho$ which combined with Eq. (1) yields

$$u_*^2 = \frac{\tau}{\rho} = C_D U_{10}^2 \tag{2}$$

WN19 considered the following parameterizations of C_D where U_{10} is in m s^{-1} (see WN19 and their Table 1 for more details):

Wu (1969) (W69)

$$C_D \times 10^3 = 0.5 U_{10}^{0.5}; \quad 1 \leq U_{10} \leq 15 \tag{3}$$

Garratt (1977) (G77)

$$C_D \times 10^3 = 0.75 + 0.067 U_{10}; \quad 4 \leq U_{10} \leq 21 \tag{4}$$

Wu (1982) (W82)

$$C_D \times 10^3 = 0.8 + 0.065 U_{10}; \quad 1 \leq U_{10} \tag{5}$$

Yelland and Taylor (1996) (YT96)

$$C_D \times 10^3 = 0.29 + \frac{3.1}{U_{10}} + \frac{7.7}{U_{10}^2}; \quad 3 \leq U_{10} \leq 6 \tag{6}$$

$$C_D \times 10^3 = 0.60 + 0.070 U_{10}; \quad 6 \leq U_{10} \leq 26 \tag{7}$$

Kalnay et al. (1996) (K96)

$$C_D \times 10^3 = 1.3; \quad 0 \leq U_{10} \tag{8}$$

Large and Yeager (2004) (LY04)

$$C_D \times 10^3 = \frac{2.7}{U_{10}} + 0.142 + 0.076 U_{10}; \quad 0 \leq U_{10} \tag{9}$$

Andreas et al. (2012) (A12)

$$C_D \times 10^3 = 0.0583^2 \left(1 - \frac{0.243}{0.0583} U_{10} \right)^2; \quad 0 \leq U_{10} \tag{10}$$

All these C_D models are valid for neutral stability of the atmosphere.

In summary, Eq. (2) using Eqs. (3)–(10) is provided in Table 1 by defining $u \equiv U_{10}$ and $T \equiv \tau/\rho$ referred to as models 1–7. More specifically, Eq. (2) using Eq. (3) is referred to as model 1 and is represented as

$$T(u) \times 10^3 = f u^g \tag{11}$$

where the coefficients f, g are given in Table 1. Furthermore, Eq. (2) using Eqs. (4)–(10) are referred to as models 2–7, respectively, and are represented as

$$T(u) \times 10^3 = a + bu + cu^2 + du^3 + eu^4 \tag{12}$$

where the coefficients a, b, c, d, e are given in Table 1.

3. Estimating wind stress using wind statistics

Parametric models for the cumulative distribution function (*cdf*) (or the probability density function (*pdf*)) of $u = U_{10}$ are provided in the literature, see for example a review by Bitner-Gregersen (2015). In the present study results are exemplified using four *cdfs* of u ; one from Johannessen et al. (2001), two from Mao and Rychlik (2017) and one from Li et al. (2015). The first *cdf* of u is based on one-hourly values of u from wind measurements covering the years 1973–1999 from the Northern North Sea (NNS) (see Johannessen et al. (2001) for more details). The next two *cdfs* of u represent the wind speed at two locations along a ship route in the North Atlantic (NA) with coordinates 20°W 60°N (South of Iceland) and coordinates 10°W 40°N (see also Figure 2 in WN19) fitted to 10 years of wind speed data (see Mao and Rychlik (2017) for more details). The last *cdf* of u represents the wind speed obtained as best fit to hindcast wind data from 2001–2010 at the Buoy Cabo Silleiro location 40 km off the North-West Spanish coast (see Li et al. (2015) for more details). All these *cdfs* are given by the two-parameter Weibull model

Table 1 Wind stress formulae and coefficients according to Eq. (11) for model 1 and Eq. (12) for models 2–7.

Model, Eq. number	Authors	a	b	c	d	e	f	g	u_1 [m s ⁻¹]	u_2 [m s ⁻¹]	u_3 [m s ⁻¹]
1, Eq. (11)	W69	-	-	-	-	-	0.5	2.5	1	-	15
2, Eq. (12)	G77	-	-	0.75	0.067	-	-	-	4	-	21
3, Eq. (12)	W82	-	-	0.8	0.065	-	-	-	1	-	∞
4, Eq. (12)	YT96	7.7	3.1	0.29	-	-	-	-	3	6	-
		-	-	0.60	0.070	-	-	-	-	6	26
5, Eq. (12)	K96	-	-	1.3	-	-	-	-	0	-	∞
6, Eq. (12)	LY04	-	2.7	0.142	0.076	-	-	-	0	-	∞
7, Eq. (12)	A12	-	-	0.0034	-0.0283	0.059	-	-	0	-	∞

Table 2 Wind stress results using wind statistics from NA (20°W 60°N) and NNS (the results for $E[T]$ and $E[T] \pm 1 SD$ are multiplied by 10³).

Model number	NA (20°W 60°N)					NNS				
	$E[T]$ [m ² s ⁻²]	$R[T]$	$E[T] - 1 SD$ [m ² s ⁻²]	$E[T] + 1 SD$ [m ² s ⁻²]	$\frac{T(E[U_{10}])}{E[T]}$	$E[T]$ [m ² s ⁻²]	$R[T]$	$E[T] - 1 SD$ [m ² s ⁻²]	$E[T] + 1 SD$ [m ² s ⁻²]	$\frac{T(E[U_{10}])}{E[T]}$
1	144	0.78	32	256	1.03	94	1.08	0	196	0.83
2	191	0.88	23	359	0.70	147	1.07	0	304	0.48
3	187	1.02	0	378	0.73	128	1.49	0	319	0.57
4	179	0.999	0	358	0.68	135	1.29	0	309	0.47
5	147	0.82	26	268	0.84	100	1.18	0	218	0.74
6	155	1.04	0	316	0.71	105	1.54	0	267	0.58
7	1213	1.72	0	3299	0.42	807	2.86	0	3115	0.22

$$P(u) = 1 - \exp\left[-\left(\frac{u}{\theta}\right)^\beta\right]; \quad u \geq 0 \quad (13)$$

with the Weibull scale (θ) and shape (β) parameters as NNS (Johannessen et al., 2001):

$$\theta = 8.426 \text{ m s}^{-1}, \quad \beta = 1.708 \quad (14)$$

NA (20°W 60°N) (Mao and Rychlik, 2017):

$$\theta = 10.99 \text{ m s}^{-1}, \quad \beta = 2.46 \quad (15)$$

NA (10°W 40°N) (Mao and Rychlik, 2017):

$$\theta = 7.11 \text{ m s}^{-1}, \quad \beta = 2.30 \quad (16)$$

NA (Buoy Cabo Silleiro) (Li et al., 2015):

$$\theta = 7.866 \text{ m s}^{-1}, \quad \beta = 2.002 \quad (17)$$

According to the summary of the models in Table 1 they are generally valid within a finite interval of u and thus the pdf of u follows the truncated Weibull pdf:

$$p_t(u) = \frac{1}{N} p(u); \quad u_1 \leq u \leq u_3 \quad (18)$$

$$N = \exp\left[-\left(\frac{u_1}{\theta}\right)^\beta\right] - \exp\left[-\left(\frac{u_3}{\theta}\right)^\beta\right] \quad (19)$$

where

$$p(u) = \frac{dP(u)}{du} = \frac{\beta}{\theta} \left(\frac{u}{\theta}\right)^{\beta-1} \exp\left[-\left(\frac{u}{\theta}\right)^\beta\right]; \quad u_1 \leq u \leq u_3 \quad (20)$$

In the following the expected value, $E[T]$, and the variance, $Var[T]$, of the wind shear stress $T = \tau/\rho$ are calculated based on the given formulae and coefficients in

Table 1, and the wind statistics from NNS and NA. For models 1–3 and 5–7 $E[T]$ and $Var[T]$ are calculated from Eqs. (18)–(20) as (Bury, 1975, Ch. 2)

$$E[T(u)] = \int_{u_1}^{u_3} T(u) p_t(u) du \quad (21)$$

$$Var[T(u)] = E[T^2(u)] - (E[T(u)])^2 \quad (22)$$

$$E[T^2(u)] = \int_{u_1}^{u_3} T^2(u) p_t(u) du \quad (23)$$

where u_1 and u_3 are given in Table 1. For model 4 the corresponding results are calculated as

$$E[T(u)] = \int_{u_1}^{u_2} T_1(u) p_t(u) du + \int_{u_2}^{u_3} T_2(u) p_t(u) du \quad (24)$$

$$E[T^2(u)] = \int_{u_1}^{u_2} T_1^2(u) p_t(u) du + \int_{u_2}^{u_3} T_2^2(u) p_t(u) du \quad (25)$$

and $Var[T(u)]$ as in Eq. (22). Here $u_1 \leq T_1 \leq u_2$ and $u_2 \leq T_2 \leq u_3$ are as given in Table 1. One should notice that these results can be calculated analytically using the results in Appendix A.

The coefficient of variation is

$$R[T(u)] = \frac{(Var[T(u)])^{1/2}}{E[T(u)]} \quad (26)$$

The results for NNS (Eq. (14)) and NA (20°W 60°N) (Eq. (15)) for models 1–7 are given in Table 2. It should be noted that these two locations are located near the study area of WN19 (i.e. the North Atlantic and the European

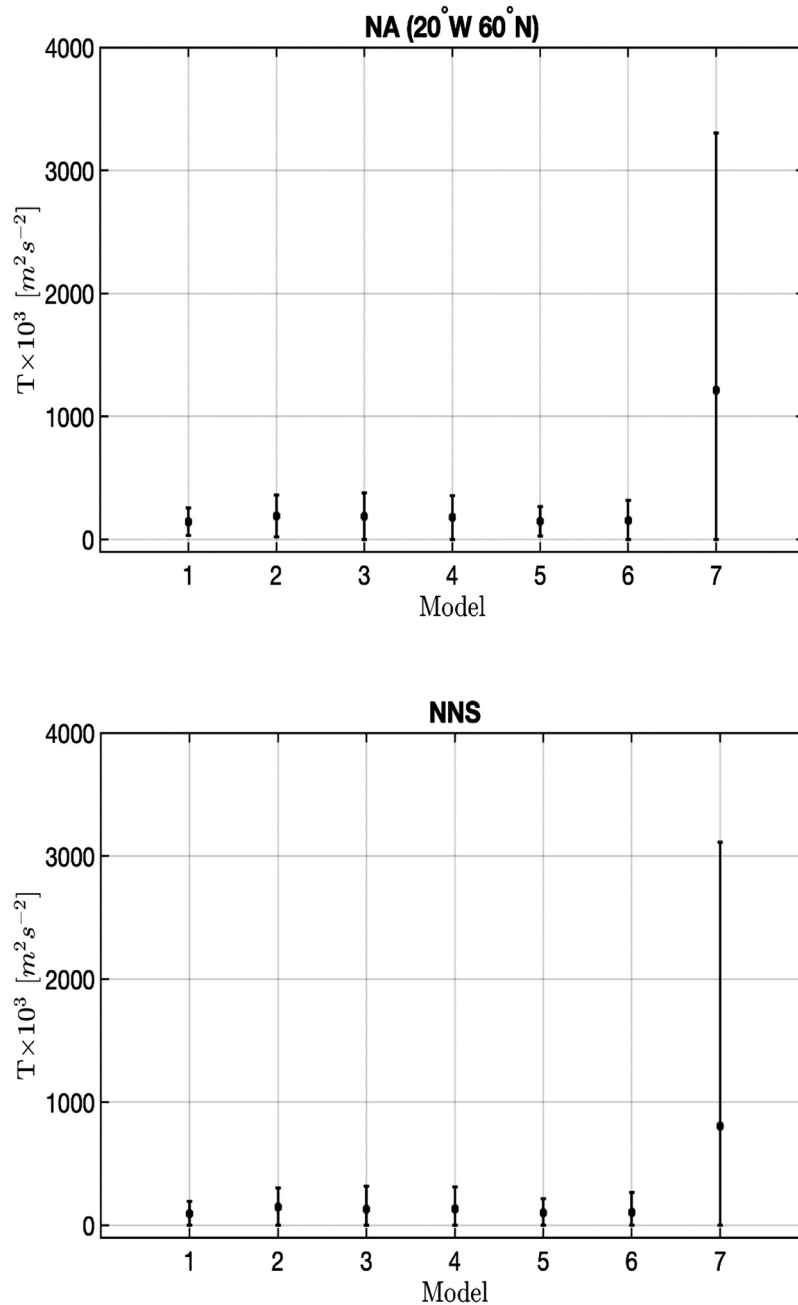


Figure 1 $E[T]$, $E[T] + 1SD$ and $E[T] - 1SD$ where $SD = (Var[T])^{1/2}$ at the NA (20°W 60°N) and NNS locations.

Arctic, see Figure 2 in WN19). Results are provided for $E[T]$, $R[T]$, $E[T]$ plus and minus one standard deviation (SD), $E[T] \pm 1SD$, where $SD = (Var[T])^{1/2} = E[T] \times R[T]$. It should be noted that the values of $E[T]$ and $E[T] \pm 1SD$ are multiplied by the factor 10^3 and all dimensions are in $m^2 s^{-2}$. From Table 2 it appears that the wind shear stress is larger at NA (20°W 60°N) than in NNS for all models with the largest value for model 7 and the smallest for model 1 at both locations. At both locations it also appears that the wind shear stress is significantly larger for model 7 compared with the other models. Moreover, the coefficients of variation $R[T]$ for all the models are large; in the range 0.78–1.72 for NA

and in the range 1.07–2.86 for NNS, i.e. reflecting large standard deviations.

The values of $E[T] \pm 1SD$ are also depicted in Figure 1. It appears from Table 2 and Figure 1 that for models 1–6 at both locations the values of $E[T]$ are within the intervals $E[T] - 1SD$ and $E[T] + 1SD$ of the other models. Although $E[T]$ for model 7 is significantly larger than those for the other models, there is overlap between the other models and the interval $E[T] - 1SD$ for model 7.

As referred to in the introduction, these results are different from those found by WN19, i.e. as they obtained the smallest wind stress using the Andreas et al. (2012) formula

Table 3 Wind stress results using wind statistics from NA (10°W 40°N) and NA (Buoy Cabo Silleiro) (the results for $E[T]$ and $E[T] \pm 1 SD$ are multiplied by 10^3).

Model number	NA (10°W 40°N)					NA (Buoy Cabo Silleiro)				
	$E[T]$ [m ² s ⁻²]	$R[T]$	$E[T] - 1 SD$ [m ² s ⁻²]	$E[T] + 1 SD$ [m ² s ⁻²]	$\frac{T(E[U_{10}])}{E[T]}$	$E[T]$ [m ² s ⁻²]	$R[T]$	$E[T] - 1 SD$ [m ² s ⁻²]	$E[T] + 1 SD$ [m ² s ⁻²]	$\frac{T(E[U_{10}])}{E[T]}$
1	69	1.03	0	140	0.72	86	1.05	0	176	0.74
2	81	0.85	12	150	0.58	113	0.997	0.3	226	0.52
3	67	1.04	0	137	0.72	93	1.22	0	206	0.66
4	70	0.89	8	132	0.59	97	1.10	0	204	0.55
5	63	0.87	8	118	0.83	80	0.999	0.1	160	0.79
6	56	0.99	0.6	111	0.75	77	1.21	0	170	0.66
7	229	1.88	0	659	0.38	433	2.26	0	1412	0.30

and the largest wind stress using the Wu (1969) formula. In order to check these results the two *cdfs* in Eqs. (16) and (17) are included representing wind conditions at locations farther south in the North Atlantic than the study area in WN19. It should be noted that the scale parameter θ (Eqs. (16) and (17)) is smaller than those in Eqs. (14) and (15), while the shape parameter β (Eqs. (16) and (17)) have values between those in Eqs. (14) and (15), reflecting different features of the wind data. Thus, similar results to those in Table 2 and Figure 1 are provided in Table 3 and Figure 2 for models 1–7 at these two NA locations (Eqs. (16) and (17)).

From Table 3 it appears that the wind shear stress is larger at NA (Buoy Cabo Silleiro) than at NA (10°W 40°N) for all models with the largest value for model 7 and the smallest for model 6 at both locations, but the wind shear stress at these locations are smaller than those at the two other locations (i.e. Table 2 and Figure 1). It is noticed that the smallest value was obtained for model 1 at the two other locations, which is attributed to the different features of the *cdfs* of the wind speed. Moreover, it also appears that the wind shear stress is significantly larger for model 7 compared with the other models at both locations. The coefficients of variation $R[T]$ are large for all the models; in the range 0.85–1.88 at NA (10°W 40°N) and in the range 0.997–2.26 at NA (Buoy Cabo Silleiro). From Table 3 and Figure 2 it also appears that for models 1–6 the values of $E[T]$ are within the intervals $E[T] - 1SD$ and $E[T] + 1SD$ of the other models at both locations, while there is overlap between the other models and the interval $E[T] - 1SD$ for model 7.

Thus, the overall results at these two locations exhibit the same main features as those obtained at NA (20°W 60°N) and in NNS, i.e. the wind shear stress is largest using model 7 (Andreas et al., 2012), while WN19 obtained the smallest shear stress using this model. The reason for this difference is unclear, but it is likely that it is partly related to how the wind data is used together with the drag coefficient, and partly to the use of global (WN19) and local (present) wind data. However, more studies are required to investigate this issue, but this is beyond the scope of this article.

An alternative to the stochastic method used here for estimating the wind shear stress is to use a deterministic method, which is to substitute $u = E[U_{10}]$ in Eqs. (11) and

(12) for models 1–7, i.e. to calculate $T(E[U_{10}])$. Here $E[U_{10}]$ is obtained using the *cdf* in Eq. (13) giving (Bury, 1975, Ch. 2)

$$E[U_{10}] = \theta \Gamma\left(1 + \frac{1}{\beta}\right) \tag{27}$$

where Γ is the gamma function. Then, this yields for NNS (Eq. (14)) $E[U_{10}] = 7.52 \text{ m s}^{-1}$;

NA (Eq. (15)) $E[U_{10}] = 9.75 \text{ m s}^{-1}$; NA (Eq. (16)) $E[U_{10}] = 6.30 \text{ m s}^{-1}$; NA (Eq. (17)) $E[U_{10}] = 6.97 \text{ m s}^{-1}$. By using this method together with the results for $E[T]$ in Tables 2 and 3, the deterministic to stochastic method ratios $T(E[U_{10}])/E[T]$ are provided in Table 2 for NNS and NA (20°W 60°N), and in Table 3 for NA (10°W 40°N) and NA (Buoy Cabo Silleiro). At all locations the ratios are smaller than one, except for model 1 at NA (20°W 60°N) where the ratio is slightly larger than one. Overall, the stochastic method should be used as the statistical features of the wind shear stress are taken into account consistently, which is not the case for the deterministic method.

4. Summary and conclusions

A summary and the main conclusion are as follows:

The effect of the air-sea drag coefficient on estimating wind stress based on wind statistics are demonstrated. This was achieved applying the same seven wind stress bulk formulae chosen by Wrobel-Niedzwiecka et al. (2019) together with mean wind speed statistics from three locations in NA and one location in NNS. Results are given in terms of expected values ($E[T]$) and standard deviations (SD) of the wind stress.

The wind stress is larger at NA (20°W 60°N) than in NNS for all formulae with the largest value resulting by using the Andreas et al. (2012) formula and the smallest by using the Wu (1969) formula at both these locations near the study area of Wrobel-Niedzwiecka et al. (2019). Two other data sets from locations farther south in NA are used to check the results, which confirms that the largest wind stress is obtained using the Andreas et al. (2012) formula, while the smallest is obtained using the Large and Yeager (2004) formula. Moreover, at all locations the standard deviations of the wind stress are large; $E[T]$ are within the intervals

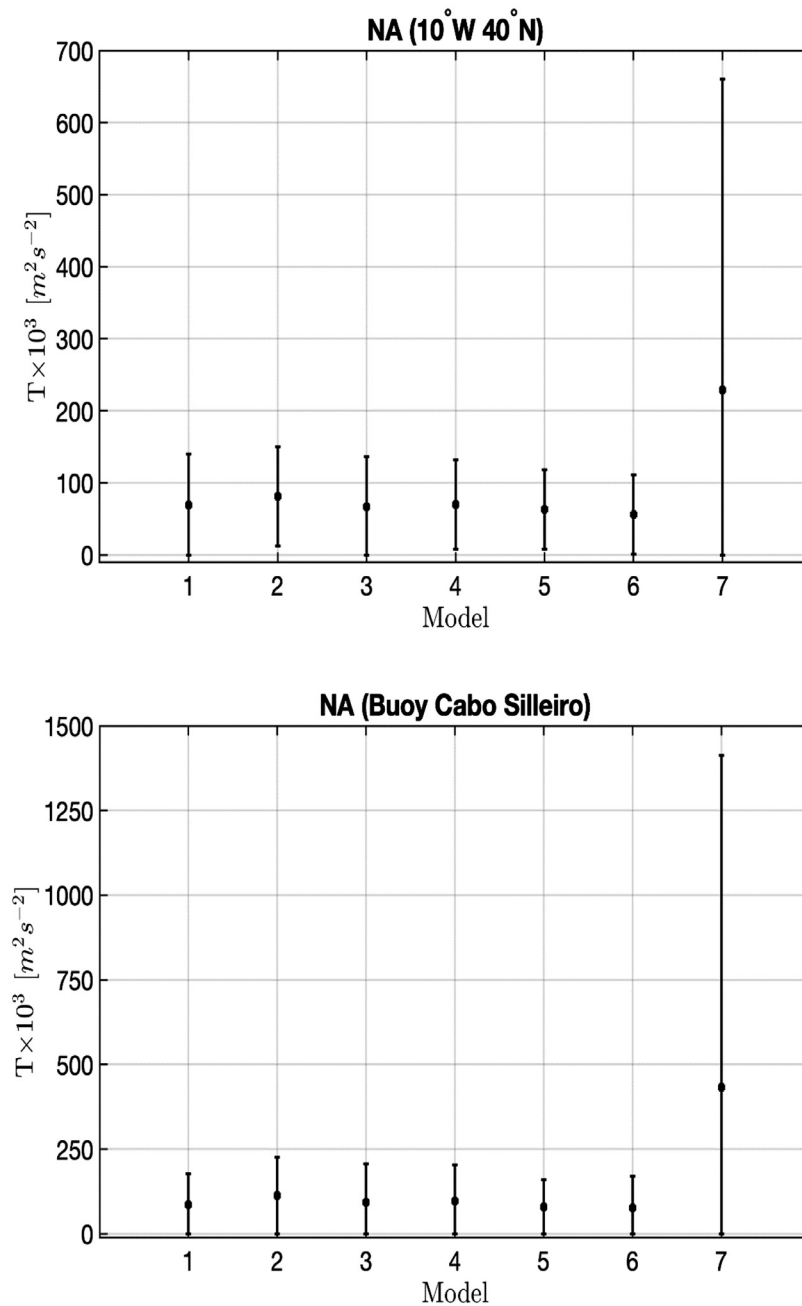


Figure 2 $E[T]$, $E[T] + 1SD$ and $E[T] - 1SD$ where $SD = (Var[T])^{1/2}$ at the NA (10°W 40°N) and NA (Buoy Cabo Silleiro) locations.

$E[T] - 1SD$ and $E[T] + 1SD$ using the other formulae, except for the [Andreas et al. \(2012\)](#) formula for which there is overlap between the interval $E[T] - 1SD$ and the intervals of the other formulae.

These results are different from those obtained by [Wrobel-Niedzwiecka et al. \(2019\)](#) where the smallest wind stress resulted from using the [Andreas et al. \(2012\)](#) formula and the largest wind stress by using the [Wu \(1969\)](#) formula. The difference is probably attributed to how the wind data is used in combination with the drag coefficient and to the use of global ([Wrobel-Niedzwiecka et al., 2019](#)) and local (present) wind data. However, this is not conclusive and needs further investigations.

The present stochastic method should be used rather than the deterministic one since the statistical features of the wind stress are then taken into account in a consistent way.

Appendix A

Let $p_t(u)$ denote the truncated pdf in [Eqs. \(18\)–\(20\)](#). Then $E[T]$ and $Var[T]$ in [Eqs. \(21\)–\(25\)](#) can be calculated analytically using the results provided in [Abramowitz and Stegun \(1972, Chs. 6.5 and 26.4\)](#).

For models 1 and 2 the calculations contain terms like:

$$E[u^n] = \int_{u_1}^{u_3} u^n p_t(u) du = \frac{1}{N} \theta^n \left\{ \Gamma \left[1 + \frac{n}{\beta}, \left(\frac{u_1}{\theta} \right)^\beta \right] - \Gamma \left[1 + \frac{n}{\beta}, \left(\frac{u_3}{\theta} \right)^\beta \right] \right\} \quad (A1)$$

where Γ is the gamma function, $\Gamma(x, y)$ is the incomplete gamma function, n is a real number (not necessarily an integer), $\Gamma(x, 0) = \Gamma(x)$ and $\Gamma(x, \infty) = 0$.

For model 3 the calculations contain terms like (i.e. for $u_3 \rightarrow \infty$ in Eq. (A1)):

$$E[u^n] = \int_{u_1}^{\infty} u^n p_t(u) du = \frac{1}{N} \theta^n \Gamma \left[1 + \frac{n}{\beta}, \left(\frac{u_1}{\theta} \right)^\beta \right] \quad (A2)$$

For model 4 the calculations contain terms like:

$$E[u^n] = \int_{u_1}^{u_2} u^n p_t(u) du = \frac{1}{N} \theta^n \left\{ \Gamma \left[1 + \frac{n}{\beta}, \left(\frac{u_1}{\theta} \right)^\beta \right] - \Gamma \left[1 + \frac{n}{\beta}, \left(\frac{u_2}{\theta} \right)^\beta \right] \right\} \quad (A3)$$

$$E[u^n] = \int_{u_2}^{u_3} u^n p_t(u) du = \frac{1}{N} \theta^n \left\{ \Gamma \left[1 + \frac{n}{\beta}, \left(\frac{u_2}{\theta} \right)^\beta \right] - \Gamma \left[1 + \frac{n}{\beta}, \left(\frac{u_3}{\theta} \right)^\beta \right] \right\} \quad (A4)$$

One should notice that in both Eqs. (A3) and (A4), $p_t(u)$ and N are as given in Eqs. (18) and (19), respectively.

For models 5, 6 and 7 the calculations contain terms like (i.e. using the Weibull pdf without truncation corresponding to $u_1 = 0$, $u_3 \rightarrow \infty$ in Eq. (A1)):

$$E[u^n] = \int_0^{\infty} u^n p(u) du = \theta^n \Gamma \left(1 + \frac{n}{\beta} \right) \quad (A5)$$

References

Abramowitz, M., Stegun, I.A., 1972. *Handbook of Mathematical Functions*. Dover Publications, New York, 1046 pp.

Andreas, E.L., Mahrt, L., Vickers, D., 2012. A new drag relation for aerodynamically rough flow over the ocean. *J. Atmos. Sci.* 69 (8), 2520–2539. <https://doi.org/10.1175/JAS-D-11-0312.1>

Bitner-Gregersen, E.M., 2015. Joint met-ocean description for design and operations of marine structures. *Appl. Ocean Res.* 51, 279–292. <https://doi.org/10.1016/j.apor.2015.01.007>

Bury, K.V., 1975. *Statistical Models in Applied Science*. John Wiley & Sons, New York, 646 pp.

Garratt, J.R., 1977. Review of drag coefficients over oceans and continents. *Mon. Weather Rev.* 105 (7), 915–929. [https://doi.org/10.1175/1520-0493\(1977\)105<0915:RODCOO>2.0.CO;2](https://doi.org/10.1175/1520-0493(1977)105<0915:RODCOO>2.0.CO;2)

Johannessen, K., Meling, T.S., Haver, S., 2001. Joint distribution of wind and waves in the Northern North Sea. In: Chung, J.S., Prevosto, M., Mizutani, N. (Eds.), *Proceedings of the 11th Int. Offshore and Polar Engineering Conf.*, Stavanger, Norway. Int. Soc. Offshore and Polar Engineer (ISOPE), Cupertino, CA, USA, Vol. 3, 19–28.

Kalnay, E., Kanamitsu, M., Kistler, R., Collins, W., Daeven, D., Gandin, L., Iredell, M., Saha, S., White, G., Woollen, J., Zhu, Y., Chelliah, M., Ebisuzaki, W., Higgins, W., Janowiak, J., Mo, K.C., Ropelewski, S., Wang, J., Leetmaa, A., Reynolds, R., Jenne, R., Joseph, D., 1996. The NCEP/NCAR 40-year reanalysis project. *Bull. Am. Meteor. Soc.* 77 (3), 437–471.

Large, W.G., Yeager, S.G., 2004. Diurnal to decadal global forcing for ocean and sea-ice models: the data sets and flux climatologies. *Technical Note NCAR/TN-460 + STR*. NCAR, Boulder, CO.

Li, L., Gao, Z., Moan, T., 2015. Joint distribution of environmental condition at five European offshore sites for design of combined wind and wave energy devices. *J. Offshore Mech. Arct. Eng.* 137 (3), 031901. <https://doi.org/10.1115/1.4029842>

Mao, W., Rychlik, I., 2017. Estimation of Weibull distribution for wind speeds along ship routes. *Proceedings of the Institution of Mechanical Engineers, Part M: J. Eng. Maritime Environ.* 231 (2), 464–480. <https://doi.org/10.1177/1475090216653495>

Wrobel-Niedzwiecka, I., Drozdowska, V., Piskozub, J., 2019. Effect of drag coefficient formula choice on wind stress climatology in the North Atlantic and the European Arctic. *Oceanologia* 61 (3), 291–299. <https://doi.org/10.1016/j.oceano.2019.02.002>

Wu, J., 1969. Wind stress and surface roughness at air-sea interface. *J. Geophys. Res.* 74 (2), 444–455. <https://doi.org/10.1029/JB074i002p00444>

Wu, J., 1982. Wind-stress coefficients over sea surface from breeze to hurricane. *J. Geophys. Res.* 87 (C12), 9704–9706. <https://doi.org/10.1029/JC087i12p09704>

Yelland, M., Taylor, P.K., 1996. Wind stress measurements from the open ocean. *J. Phys. Oceanogr.* 26 (4), 541–558. [https://doi.org/10.1175/1520-0485\(1996\)026<0541:WSMFTO>2.0.CO;2](https://doi.org/10.1175/1520-0485(1996)026<0541:WSMFTO>2.0.CO;2)